PAPER • OPEN ACCESS

Nonlinear optically detected electrophonon resonance full width at half maximum in a parabolic GaAs quantum well with different phonon models

To cite this article: Nguyen Dinh Hien *et al* 2019 *J. Phys.: Conf. Ser.* **1274** 012011

IOP Conf. Series: Journal of Physics: Conf. Series **1274** (2019) 012011 doi:10.1088/1742-6596/1274/1/012011

Nonlinear optically detected electrophonon resonance full width at half maximum in a parabolic GaAs quantum well with different phonon models

Nguyen Dinh Hien[1,2], Nguyen Trung Dung[3], Le Dinh[4], Tran Cong Phong[5]

[1]Laboratory of Magnetism and Magnetic Materials, Advanced Institute of Materials Science, Ton Duc Thang University, Ho Chi Minh City, Viet Nam.
[2]Faculty of Applied Sciences, Ton Duc Thang University, Ho Chi Minh City, Viet Nam.
[3]Nghen High School, Can Loc Town, Ha Tinh Province, Viet Nam.
[4]Center for Theoretical & Computational Physics, Hue University's College of Education, No. 34, Le Loi Str., Hue City, Viet Nam.
[5]Viet Nam Institute of Educational Sciences, 101 Tran Hung Dao Str., Ha Noi, Viet Nam.

E-mail: nguyendinhhien@tdtu.edu.vn (Nguyen Dinh Hien)

Abstract.
The effect of different phonon models (confined and bulk phonons) on the linear optically detected electrophonon resonance (LODEPR), nonlinear optically detected electron-phonon resonance (NLODEPR) effect and full-width at half-maximum (FWHM) of the LODEPR and NLODEPR peaks via both one and two photon absorption processes in a parabolic GaAs quantum well by using the state-dependent operator projection is theoretically studied. The obtained numerical result for the parabolic GaAs/AlAs quantum well shows that the FWHM of the LODEPR and NLODEPR peaks increase with increasing well's confinement frequency and temperature for the above both models of the phonon. Besides, the FWHM of the LODEPR and NLODEPR peaks for the confined phonon case varies faster and have a larger value than it does for the bulk phonon case. Furthermore, the FWHM of the NLODEPR peaks is about one order of value smaller than the linear one for the above both models of the phonon; in the large range of the confinement frequency ($\omega_z/\omega_{LO} > 0.2$), the effect of phonon confinement on the FWHM of the LODEPR and NLODEPR peaks becomes important and cannot be neglected in considering.

1. Introduction

The electrophonon resonance (EPR) phenomena arises from an electron scattering due to the absorption and/or emission of phonons whenever the longitudinal optical phonon energy is equal to the energy separation between two electric subband levels [1, 2]. This effect shows one of the typical characteristics of low-dimensional electron systems that can not be observed in bulk materials. The EPR and the optically detected electrophonon resonance (ODEPR) provide useful information on relative transport properties of semiconductors, such as the scattering mechanism of carriers, including the effective mass, the energy difference between electric subband levels, and the electron-phonon interactions [2]. The two-photon absorption is a nonlinear process in which tow photons of identical or different frequencies are simultaneously absorbed by the same species exciting the molecule from one state to a higher energy electronic state. In materials with an elastic arrangement of atoms or molecules there exist phonons (quanta of lattice vibration), this process may involve the absorption and/or emission phonons. It is a nonlinear process and is different considerably from the one-photon absorption process which is related linearly to the intensity of light. The confine phonon causes the increase of electron-phonon scattering rates [3, 4] and modifies the phonon density of states [5]. The confine phonon effect is shown to be important whenever confinement lengths are smaller than the phonon coherence length [3] and should be taken into account in order to obtain realistic estimates for electron-phonon interaction in low-dimensional structures [7]. There are several confined phonon mode models due to different lattice dynamics boundary conditions in low-dimensional structures, such as the Huang-Zhu model (both electric potential and polarization have nodes at the interfaces), the slab mode model (when the electric potential has nodes at the interface and the in-plane component of phonon wave vector is much larger than its quantized one) and the guided mode model (the opposite limit as the slab mode) [6, 12]. However, the HZ model has received wide acceptance and best describes and been in good agreement with experimental results [14]. The FWHM is well-known as a good tool for investigating the scattering mechanisms of carriers. Hence, it can be used to probe electron-phonon scattering processes. The FWHM is defined as the profile of curves describing the dependence of the absorption power on the phonon energy or frequency [8]. The FWHM has been measured in various kinds of semiconductors, such as quantum wells [9], quantum wires [10], and quantum dots [11]. These results show that the FWHM has a weak dependence on temperature and has a strong dependence on the sample size. However, in these studies, the FWHM was investigated based on the interaction of electrons and bulk phonons. In the case of confined phonon, many works have been reported to clarify the effect of different phonon models on the electron-phonon scattering rates [12], free carrier absorption [13], energy loss rate of hot electrons [14], localized phonon-assisted cyclotron resonance [15], [16], self-energy of confined polaron [17], electron-phonon interaction energies [18], optically detected electron-phonon resonance [19], optically detected magneto-phonon resonance [20]. So that, the absorption FWHM in a parabolic quantum well due to confined optical phonon-electron interaction has not been fully considered in previously published reports. Recently, our group has proposed a method, called the profile method. This method can be used to computationally obtain the FWHM from graphs of the absorption power [21], we used this method to determine the cyclotron resonance FWHM in cylindrical quantum wires [22], the effect of phonon confinement on the optically detected electrophonon resonance FWHM in GaAs/AlAs quantum wires [23, 24], the effect of phonon confinement on the optically detected magneto phonon resonance FWHM in quantum wells [20], and the confine optical-phonon-assisted cyclotron resonance in quantum wells via two-photon absorption process [25]. The study of two-photon absorption process has been admitted to be important for in-depth understanding the transient response of semiconductors excited by an electromagnetic field. Especially, in applied optics, two-photon absorption in semiconductors has been suggested as a replacement nonlinear process for autocorrelation measurements [26]. Therefore, the two-photon absorption process has been examined in several works. Bristow et al. [27] have measured the degenerate two-photon absorption and Kerr coefficient of bulk Si. The linear and nonlinear optical response via two-photon absorption of asymmetric GaAs/GaAlAs quantum wells [28], in multiple quantum wells [29], in a GaAs quantum wires [30], confined optical-phonon-assisted cyclotron resonance in quantum wells via two-photon absorption process [25], and in a GaAs/AlGaAs single quantum dot [31] have also been presented. However, the two-photon absorption process by electrons scattered by confine phonons in a parabolic quantum well has not been fully considered in previously published reports. So, the effect of phonon confinement in a parabolic quantum well as well as multi-photon processes need to be considered.

In the present work, we investigate effect of confined phonons on the FWHM of the LODEPR and NLODEPR peaks in a parabolic GaAs quantum well. The dependence of the FWHM of the LODEPR and NLODEPR peaks on the well's confinement frequency and temperature of system are obtained. The results of the present work are fairly different from the previous theoretical results because the confine LO phonon described by Huang-Zhu model are considered detail, and the results are compared with the corresponding calculations for bulk phonon model. The paper is organized as follows. In Section 2, we introduce Huang-Zhu model of phonon confinement in a parabolic quantum well. Calculations of analytical expression of the absorption power in a parabolic quantum well due to confine and bulk LO phonon modes are presented in Section 3. The graphical dependence of the absorption power on the photon energy in the parabolic GaAs quantum well is shown in Section 4. From this dependence, we obtain the dependence of the FWHM of the LODEPR and NLODEPR peaks on temperature and well's confinement frequency for both bulk and confine phonon model. Finally, remarks and conclusions are shown in Section 5.

2. Huang-Zhu model of phonon confinement in parabolic quantum well

We consider a single parabolic quantum well structure, the one-electron eigenfunction, $|\alpha\rangle = \Psi_{k_\perp,n}$, is given by [2]

$$\Psi_{k_\perp,n} = \frac{1}{\sqrt{L_x L_y}} \exp(i\vec{k}_\perp \vec{r}_\perp)\varphi_n(z), \tag{1}$$

where L_x, L_y are specimen dimension in x, y-direction; $\vec{k}_\perp = (k_x, k_y)$ and $\vec{r}_\perp = (x, y)$ are the wave vector and position vector of a conduction electron in the (x, y) plane, respectively; $\varphi_n(z)$ is the electron wave function in z-direction as determined by the parabolic potential $V(z)$, $V(z) = m^*\omega_z^2 z^2/2$. The corresponding electron wave function and energy eigenvalues, $E_{n,\vec{k}_\perp}$ are given by [2]

$$\varphi_n(z) = \frac{1}{\sqrt{2^n n! \sqrt{\pi} a_z}} \exp(-\frac{z^2}{2a_z^2}) H_n(\frac{z}{a_z}), \tag{2}$$

$$E_{n,\vec{k}_\perp} = \frac{\hbar^2 k_\perp^2}{2m^*} + (n + \frac{1}{2})\hbar\omega_z, \tag{3}$$

where $n = 0, 1, 2, \cdots$ is the electric subband quantum number; m^* and ω_z are the effective mass of an electron and well's confinement frequency, respectively. In this case $\varphi_n(z)$ is given by [2]

$$\varphi_n(z) = \frac{1}{\sqrt{2^n n! \sqrt{\pi} a_z}} \exp(-\frac{z^2}{2a_z^2}) H_n(\frac{z}{a_z}), \tag{4}$$

with $a_z = (\hbar/(m^*\omega_z))^{1/2}$, and H_n are Hermite polynomials of order n.

The matrix element for electron-confined phonon interaction in parabolic quantum well in the extreme quantum limits can be written as [32]

$$|\langle i|H_{e-ph}|f\rangle|^2 = \frac{e^2\hbar\omega_{LO}\chi^*}{2\epsilon_0 V_0} |V_{m\theta}^{\nu}(q_\perp)|^2 |G_{n_i,n_f}^{\nu,m\theta}|^2 \delta_{k_\perp^f, k_\perp^i \pm q_\perp}, \tag{5}$$

where the overlap integral, $G_{n_i,n_f}^{m\phi}$, is given

$$G_{n_i,n_f}^{m\phi} = \int_{-\infty}^{\infty} \varphi_{n_f}^*(z) u_{m\phi}(z) \varphi_{n_i}(z) dz, \tag{6}$$

where $\chi^* = (\chi_\infty^{-1} - \chi_0^{-1})$ with χ_∞ and χ_0 are the high and static-frequency dielectric constants, respectively; ϵ_0 is the vacuum dielectric constants, and $V_0 = SL_z$ is the volume of the system;

$u^{HZ}_{m\phi}(z)$ is the parallel component of the displacement vector of $m-$th phonon mode in the direction of the spatial confinement for the HZ model (HZ) [33]; ϕ are the even $(-)$ and odd $(+)$ HZ model phonons. In the next section, we will use the HZ model to calculate the optical absorption power in parabolic quantum well. For this model, $u^{HZ}_{m\phi}(z)$, is given by

$$u^{HZ}_{m+}(z) = \sin(\frac{\mu_m \pi z}{L_z}) + \frac{c_m z}{L_z},\ m = 3,5,7,\cdots, \tag{7}$$

$$u^{HZ}_{m-}(z) = \cos(\frac{\mu_m \pi z}{L_z}) - (-1)^{m/2},\ m = 2,4,6,\cdots, \tag{8}$$

with μ_m are successive solutions of the equation

$$\tan(\frac{\mu_m \pi}{2}) = \frac{\mu_m \pi}{2},\ m-1 < \mu_m < m, \tag{9}$$

and c_m are given by

$$c_m = -2\sin(\frac{\mu_m \pi}{2}). \tag{10}$$

3. Analytical results for optical absorption power in a parabolic quantum well

Nonlinear absorption power with the HZ model of confined phonon in parabolic quantum well can be written as follows:

$$P_{NLn}(\omega) = \frac{E_0^2}{2} Re\{\sigma_{NLn}(\omega)\}, \tag{11}$$

where E_0 and ω are amplitude and frequency of external electric field; $Re\{\sigma_{NLn}(\omega)\}$ is the real part of the optical conductivity tensor, $\sigma_{NLn}(\omega)$, which is expressed in the lowest-order nonlinear form by

$$\sigma_{NLn}(\omega) = \sigma_{ij}(\omega) + \sum_k \sigma_{ijk}(\omega) E_k(\omega), \tag{12}$$

where the Latin symbols i, j and k stand for x, y and z components of the Cartesian coordinates; $\sigma_{ij}(\omega)$ being the linear conductivity tensor; $\sigma_{ijk}(\omega)$ being the component of the nonlinear conductivity tensor.

From Eq. (12) we obtain

$$Re\{\sigma_{NLn}(\omega)\} = Re\{\sigma_{zz}(\omega)\} + Re\{\sigma_{zzz}(\omega) E_z(\omega)\}. \tag{13}$$

In Eq. (13), the first and the second term correspond to the linear and nonlinear terms of the conductivity tensor, given as follows, respectively; $E_z(\omega)$ being the component of external electric field applied along the z-direction.

$$Re\{\sigma_{zz}(\omega)\} = e \sum_{\alpha,\beta} (z)_{\alpha\beta} (j_z)_{\beta\alpha} \frac{(f_\alpha - f_\beta) B_0^{\alpha\beta}(\omega)}{(\hbar\omega - E_{\alpha\beta})^2 + [B_0^{\alpha\beta}(\omega)]^2}, \tag{14}$$

where e being the electric charge of electron,

$$Re\{\sigma_{zzz}(\omega)\} = e^2 \sum_{\alpha,\beta} N_0 \quad \Big\{ \textstyle\sum_\gamma (-N_1)[(\hbar\omega - E_{\beta\alpha}) B_1(2\omega) + B_0(\omega)(2\hbar\omega - E_{\beta\gamma})]$$
$$+ \textstyle\sum_\delta N_2[(\hbar\omega - E_{\beta\alpha}) B_2(2\omega) + B_0(\omega)(2\hbar\omega - E_{\delta\alpha})] \Big\}, \tag{15}$$

where

$$N_0 = \frac{(z)_{\alpha\beta}(f_\beta - f_\alpha)}{(\hbar\omega - E_{\beta\alpha})^2 + [B_0(\omega)]^2}, \tag{16}$$

$$N_1 = -\frac{i(z)_{\gamma\alpha}(j_z)_{\beta\gamma}}{(2\hbar\omega - E_{\beta\gamma})^2 + [B_1(2\omega)]^2}, \tag{17}$$

$$N_2 = -\frac{i(z)_{\beta\delta}(j_z)_{\delta\alpha}}{(2\hbar\omega - E_{\delta\alpha})^2 + [B_2(2\omega)]^2}, \tag{18}$$

$$(z)_{\alpha\beta} = a_z\left(\sqrt{\frac{n_\beta+1}{2}}\delta_{n_\alpha,n_\beta+1} + \sqrt{\frac{n_\beta}{2}}\delta_{n_\alpha,n_\beta-1}\right)\delta_{k_{\perp\beta},k_{\perp\alpha}}, \tag{19}$$

$$(j_z)_{\beta\alpha} = \frac{ie\hbar}{m^* a_z}\left(\sqrt{\frac{n_\alpha}{2}}\delta_{n_\beta,n_\alpha-1} - \sqrt{\frac{n_\alpha+1}{2}}\delta_{n_\beta,n_\alpha+1}\right)\delta_{k_{\perp\beta},k_{\perp\alpha}}, \tag{20}$$

f_α and f_β are the Fermi-Dirac distribution function of the electron at state $|\alpha\rangle$ and $|\beta\rangle$,

$$B_0^{\alpha\beta}(\omega) = \tag{21}$$

$$\begin{aligned} C_0\sum_{n_\eta}\sum_{m,\phi=\pm} &\Bigg\{\frac{2m^*k_{1+}^2|G^{HZ,m\phi}_{n_\alpha n_\eta}|^2}{\hbar^2|k_{1+}|(a_{m\phi}k_{1+}^2+\frac{b_{m\phi}}{L_z^2})}[(1+N_q)f_\beta(1-f_{\eta,k_{1+}}) - N_q f_{\eta,k_{1+}}(1-f_\beta)] \\ &+\frac{2m^*k_{1-}^2|G^{HZ,m\phi}_{n_\alpha n_\eta}|^2}{\hbar^2|k_{1-}|(a_{m\phi}k_{1-}^2+\frac{b_{m\phi}}{L_z^2})}[N_q f_\beta(1-f_{\eta,k_{1-}}) - (1+N_q)f_{\eta,k_{1-}}(1-f_\beta)] \\ &+\frac{2m^*k_{2+}^2|G^{HZ,m\phi}_{n_\beta n_\eta}|^2}{\hbar^2|k_{2+}|(a_{m\phi}k_{2+}^2+\frac{b_{m\phi}}{L_z^2})}[(1+N_q)f_{\eta,k_{2+}}(1-f_\alpha) - N_q f_\alpha(1-f_{\eta,k_{2+}})] \\ &+\frac{2m^*k_{2-}^2|G^{HZ,m\phi}_{n_\beta n_\eta}|^2}{\hbar^2|k_{2-}|(a_{m\phi}k_{2-}^2+\frac{b_{m\phi}}{L_z^2})}[N_q f_{\eta,k_{2-}}(1-f_\alpha) - (1+N_q)f_\alpha(1-f_{\eta,k_{2-}})]\Bigg\}, \end{aligned} \tag{22}$$

$$B_1^{\alpha\beta\gamma}(2\omega) =$$

$$\begin{aligned} C_0\sum_{n_\eta}\sum_{m,\phi=\pm} &\Bigg\{\frac{2m^*k_{3+}^2|G^{HZ,m\phi}_{n_\gamma n_\eta}|^2}{\hbar^2|k_{3+}|(a_{m\phi}k_{3+}^2+\frac{b_{m\phi}}{L_z^2})}[N_q f_{\eta,k_{3+}}(1-f_\beta) - (1+N_q)f_\beta(1-f_{\eta,k_{3+}})] \\ &+\frac{2m^*k_{3+}^2|G^{HZ,m\phi}_{n_\gamma n_\eta}|^2}{\hbar^2|k_{3+}|(a_{m\phi}k_{3+}^2+\frac{b_{m\phi}}{L_z^2})}[(1+N_q)f_\alpha(1-f_{\eta,k_{3+}}) - N_q f_{\eta,k_{3+}}(1-f_\alpha)] \\ &+\frac{2m^*k_{3-}^2|G^{HZ,m\phi}_{n_\gamma n_\eta}|^2}{\hbar^2|k_{3-}|(a_{m\phi}k_{3-}^2+\frac{b_{m\phi}}{L_z^2})}[N_q f_\alpha(1-f_{\eta,k_{3-}}) - (1+N_q)f_{\eta,k_{3-}}(1-f_\alpha)] \\ &+\frac{2m^*k_{3-}^2|G^{HZ,m\phi}_{n_\gamma n_\eta}|^2}{\hbar^2|k_{3-}|(a_{m\phi}k_{3-}^2+\frac{b_{m\phi}}{L_z^2})}[(1+N_q)f_{\eta,k_{3-}}(1-f_\beta) - N_q f_\beta(1-f_{\eta,k_{3-}})] \\ &+\frac{2m^*k_{4-}^2|G^{HZ,m\phi}_{n_\eta n_\beta}|^2}{\hbar^2|k_{4-}|(a_{m\phi}k_{4-}^2+\frac{b_{m\phi}}{L_z^2})}[N_q f_{\eta,k_{4-}}(1-f_\alpha) - (1+N_q)f_\alpha(1-f_{\eta,k_{4-}})] \\ &+\frac{2m^*k_{4+}^2|G^{HZ,m\phi}_{n_\eta n_\beta}|^2}{\hbar^2|k_{4+}|(a_{m\phi}k_{4+}^2+\frac{b_{m\phi}}{L_z^2})}[(1+N_q)f_{\eta,k_{4+}}(1-f_\alpha) - N_q f_\alpha(1-f_{\eta,k_{4+}})]\Bigg\}, \end{aligned} \tag{23}$$

$$B_2^{\alpha\beta\delta}(2\omega) =$$

$$C_0\sum_{n_\eta}\sum_{m,\phi=\pm} \Bigg\{\frac{2m^*k_{5+}^2|G^{HZ,m\phi}_{n_\eta n_\delta}|^2}{\hbar^2|k_{5+}|(a_{m\phi}k_{5+}^2+\frac{b_{m\phi}}{L_z^2})}[(1+N_q)f_{\eta,k_{5+}}(1-f_\beta) - N_q f_\beta(1-f_{\eta,k_{5+}})]$$

$$+\frac{2m^*k_{5+}^2|G_{n_\eta n_\delta}^{HZ,m\phi}|^2}{\hbar^2|k_{5+}|(a_{m\phi}k_{5+}^2+\frac{b_{m\phi}}{L_z^2})}[N_qf_\alpha(1-f_{\eta,k_{5+}})-(1+N_q)f_{\eta,k_{5+}}(1-f_\alpha)]$$
$$+\frac{2m^*k_{5-}^2|G_{n_\eta n_\delta}^{HZ,m\phi}|^2}{\hbar^2|k_{5-}|(a_{m\phi}k_{5-}^2+\frac{b_{m\phi}}{L_z^2})}[(1+N_q)f_\alpha(1-f_{\eta,k_{5-}})-N_qf_{\eta,k_{5-}}(1-f_\alpha)]$$
$$+\frac{2m^*k_{5-}^2|G_{n_\eta n_\delta}^{HZ,m\phi}|^2}{\hbar^2|k_{5-}|(a_{m\phi}k_{5-}^2+\frac{b_{m\phi}}{L_z^2})}[N_qf_{\eta,k_{5-}}(1-f_\beta)-(1+N_q)f_\beta(1-f_{\eta,k_{5-}})]$$
$$+\frac{2m^*k_{6-}^2|G_{n_\alpha n_\eta}^{HZ,m\phi}|^2}{\hbar^2|k_{6-}|(a_{m\phi}k_{6-}^2+\frac{b_{m\phi}}{L_z^2})}[(1+N_q)f_{\eta,k_{6-}}(1-f_\beta)-N_qf_\beta(1-f_{\eta,k_{6-}})]$$
$$+\frac{2m^*k_{6+}^2|G_{n_\alpha n_\eta}^{HZ,m\phi}|^2}{\hbar^2|k_{6+}|(a_{m\phi}k_{6+}^2+\frac{b_{m\phi}}{L_z^2})}[(1+N_q)f_\beta(1-f_{\eta,k_{6+}})-N_qf_{\eta,k_{6+}}(1-f_\beta)]\Big\}, \quad (24)$$

with

$$C_0=\frac{\pi e^2\hbar\omega_{LO}\chi^*}{2\epsilon_0V_0(f_\alpha-f_\beta)}, \quad (25)$$

N_q is the Planck distribution function for a confined phonon at the state $|q\rangle=|m,q_\perp\rangle$,

$$k_{1\pm}=\{-\frac{2m^*}{\hbar^2}[(n_\eta-n_\beta)\hbar\omega_z+\hbar\omega\pm\hbar\omega_{LO}^{m,q_\perp}]\}^{1/2},$$

$$k_{2\pm}=\{\frac{2m^*}{\hbar^2}[(n_\alpha-n_\eta)\hbar\omega_z+\hbar\omega\pm\hbar\omega_{LO}^{m,q_\perp}]\}^{1/2},$$

$$k_{3\pm}=\{\frac{2m^*}{\hbar^2}[(n_\beta-n_\eta)\hbar\omega_z-2\hbar\omega\mp\hbar\omega_{LO}^{m,q_\perp}]\}^{1/2},$$

$$k_{4\pm}=\{\frac{2m^*}{\hbar^2}[(n_\gamma-n_\eta)\hbar\omega_z+2\hbar\omega\pm\hbar\omega_{LO}^{m,q_\perp}]\}^{1/2},$$

$$k_{5\pm}=\{\frac{2m^*}{\hbar^2}[(n_\alpha-n_\eta)\hbar\omega_z+2\hbar\omega\pm\hbar\omega_{LO}^{m,q_\perp}]\}^{1/2},$$

$$k_{6\pm}=\{\frac{2m^*}{\hbar^2}[(n_\delta-n_\eta)\hbar\omega_z-2\hbar\omega\mp\hbar\omega_{LO}^{m,q_\perp}]\}^{1/2}.$$

4. Numerical results and Discussion

To clarify the obtained results we numerically evaluate the absorption power, $P(\omega)$, for a specific GaAs/AlAs parabolic quantum well. The absorption power is considered to be a function of the photon energy. The parameters used in our computational evaluation are as follows [34]: $\chi_\infty=10.9,\chi_0=12.9,m^*=0.067\times m_0$ (m_0 being the mass of free electron), $\hbar\omega_0=36.25$ meV, $E_0=5.0\times10^6$ Vm^{-1}. The following conclusions are obtained in the extreme quantum limit, and assuming that only the lowest subbands are occupied by the electrons: $n_\alpha=1$, $n_\beta=2$ for confined electron.

Fig. 1a) shows the dependence of the nonlinear absorption power on the photon energy for bulk phonons (solid curve), confined phonons described by the HZ model (dashed curve). The

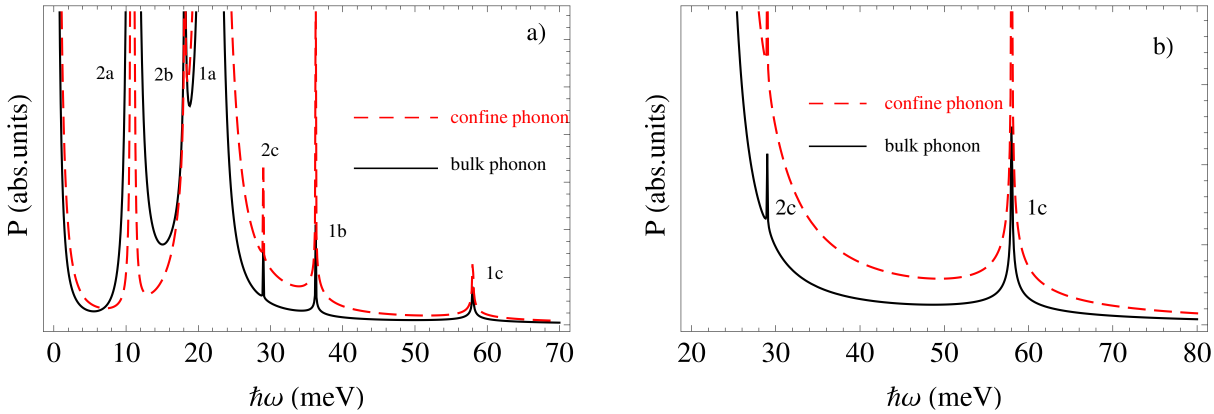

Figure 1. a) Dependence of the nonlinear absorption power in a parabolic quantum well on the photon energy for two different models of phonon: bulk phonons (the solid curve) and confined phonons (the dashed curve). Here, $T = 300$ K, and $\omega_z = 0.6\omega_{LO}$. Fig. b) is at the 2c peak (nonlinear) and 1c peak (linear) in Fig. a).

result is calculated for a parabolic quantum well, at $T = 300$ K and $\omega_z = 0.6\omega_{LO}$. There are six peaks in each curve:

- The first peak (2a) correspond to the value $\hbar\omega = 10.875$ meV, which satisfies the condition $2\hbar\omega = E_\beta - E_\alpha$. This condition implies that an electron in the $n_\alpha = 0$ can move to $n_\beta = 1$ by absorbing two photons with energy $\hbar\omega$. This is the condition for direct transitions.

- The second peak (2b) correspond to the value $\hbar\omega = 18.125$ meV, which satisfies the condition $2\hbar\omega = \hbar\omega_{LO}$. This condition implies that $n_\alpha = n_\beta$. This is the condition for intrasubband transitions.

- The third peak (1a) correspond to the value $\hbar\omega = 21.75$ meV, which satisfies the condition $\hbar\omega = E_\beta - E_\alpha$. This condition implies that an electron in the $n_\alpha = 0$ can move to $n_\beta = 1$ by absorbing a photon with energy $\hbar\omega$. This is the condition for direct transitions.

- The forth peak (2c) correspond to the value $\hbar\omega = 29.00$ meV, which satisfies the condition $2\hbar\omega = E_\beta - E_\alpha + \hbar\omega_{LO}$. This condition implies that an electron in the $n_\alpha = 0$ can move to $n_\beta = 1$ by absorbing two photons with energy $\hbar\omega$ along with emitting a phonon with the energy $\hbar\omega_{LO}$. This is the condition for nonlinear optically detected electrophonon resonance.

- The fifth peak (1b) correspond to the value $\hbar\omega = 36.25$ meV, which satisfies the condition $\hbar\omega = \hbar\omega_{LO}$. This condition implies that $n_\alpha = n_\beta$. This is the condition for intrasubband transitions.

- The sixth peak (1c) correspond to the value $\hbar\omega = 58.00$ meV, which satisfies the condition $\hbar\omega = E_\beta - E_\alpha + \hbar\omega_{LO}$. This condition implies that an electron in the $n_\alpha = 0$ can move to $n_\beta = 1$ by absorbing a photon with energy $\hbar\omega$ along with emitting a phonon with the energy $\hbar\omega_{LO}$. This is the condition for optically detected electrophonon resonance.

The third (1a), fifth (1b), sixth (1c) peaks correspond to the one-photon (linear) absorption processes. The other peaks correspond to the two-photon (nonlinear) absorption processes.

Fig. 1b) shows that the dependence of the nonlinear absorption power in a parabolic quantum well on the photon energy for two different models of phonon at the 2c peak (nonlinear) and 1c peak (linear) in 1a): bulk phonons (the solid curve) and confined phonons (the dashed curve).

Fig. 3 shows that the FWHM of the LODEPR and NLODEPR peaks increases with increasing temperature in both models of phonon. This can interpret that at high temperatures the quantity of LO-phonons linear increase with increasing temperature ($N_q \sim k_B T/\hbar\omega_{LO}$) and the electron-optical phonon interaction is dominant. Thus, when the temperature increases as the increasing FWHM, because FWHM is proportional to the possibility of electrophonon scattering. This is

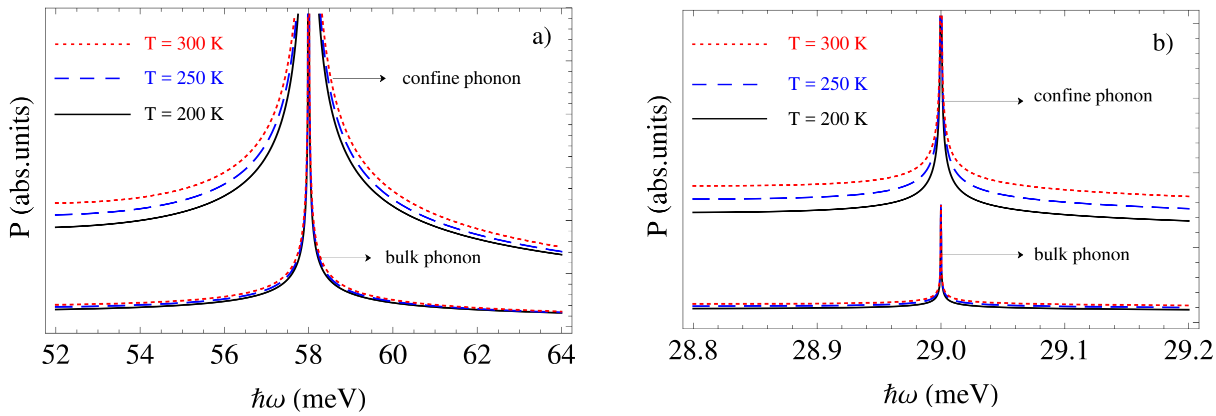

Figure 2. Dependence of the nonlinear absorption power in a parabolic quantum well on the photon energy for two different models of phonon with different values of temperature at the linear peak (Fig. a)) and nonlinear peak (Fig. b)).

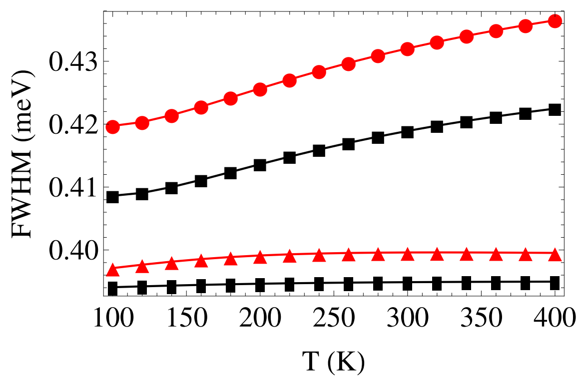

Figure 3. Dependence of the FWHM of the LODEPR and NLODEPR peaks on the temperature for two different models of phonon. The filled triangles and filled circles curves correspond to the case of bulk phonons and confined phonons for the linear absorption processes, respectively; the filled rectangles and filled squares curves correspond to the case of bulk phonons and confined phonons for the nonlinear absorption processes, respectively. Here, $\omega_z = 0.6\omega_{LO}$.

also seen the FWHM of the LODEPR and NLODEPR peaks in the case of confined phonons varies faster and has a larger value than the bulk one. This is because when phonons are confined the probability electron-phonon scattering is increased. Beside, the FWHM of the NLODEPR peak is about one order of value smaller than the linear one. This result can interpret that the contribution of two photons absorption processes to the optical absorption probability in the system is smaller than one photon absorption processes.

Fig. 4b) shows that the FWHM of the LODEPR and NLODEPR peaks increases with increasing well's confinement frequency for both models of the phonon. This can interpret that when the well's confinement frequency increases as the increasing possibility of the electron-phonon scattering, because FWHM is proportional to the possibility of electrophonon scattering. Furthermore, the FWHM of the LODEPR and NLODEPR peaks for the confined phonon case varies faster and has a larger value than it does for the bulk phonon case, and when $\omega_z/\omega_{LO} > 0.2$, the effect of confined phonon is important in study the FWHM. Physically, this is reasonable because when phonons are confined the probability electron-phonon scattering is increased. Furthermore, the FWHM of the NLODEPR peak is about one order of value smaller than the

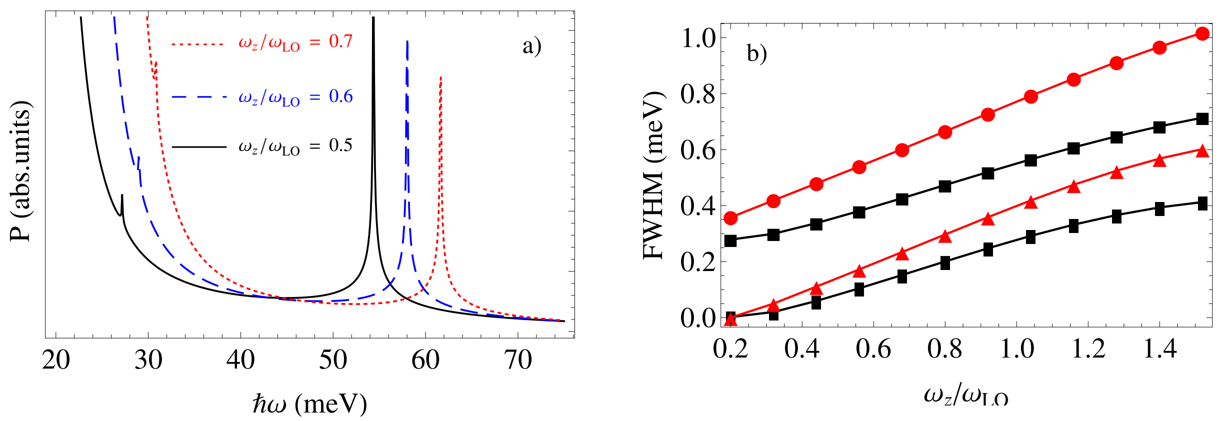

Figure 4. a) Dependence of the nonlinear absorption power in a parabolic quantum well on the photon energy with different values of the well's confinement frequency for confined phonon. b) Dependence of the FWHM of the LODEPR and NLODEPR peaks on the well's confinement frequency for two different models of phonon. The filled triangles and filled circles curves correspond to the case of bulk phonons and confined phonons for the linear absorption processes, respectively; the filled rectangles and filled squares curves correspond to the case of bulk phonons and confined phonons for the nonlinear absorption processes, respectively. Here, $T = 300$ K.

linear one. This result can interpret that the contribution of two photons absorption processes to the optical absorption probability in the system is smaller than one photon absorption processes. In addition, in the large range of the confinement frequency, the effect of phonons confinement play an important role and cannot be neglected in study the FWHM of the LODEPR and NLODEPR peaks.

5. Conclusions

We have calculated analytical expressions for the nonlinear absorption power in parabolic GaAs quantum well due to confined electrons and confined LO-phonons interaction. From the graphs of the nonlinear absorption power, we obtained the FWHM of the LODEPR and NLODEPR peaks as a profile of curves. Computational results show that in the cases of both bulk and confined phonons, the FWHM of the LODEPR and NLODEPR peaks increases with temperature and confinement frequency. Furthermore, the FWHM of the LODEPR and NLODEPR peaks for the confined phonon case has a larger value and varies faster than it does for the bulk phonon case when temperature and well's confinement frequency increase. In addition, the FWHM of the NLODEPR peak is about one order of value smaller than the linear one. Thus, in the large range of the confinement frequency ($\omega_z/\omega_{LO} > 0.2$), the effect of phonon confinement plays an important role and cannot be neglected in reaching the FWHM of the LODEPR and NLODEPR peaks. This results is the same as that obtained in a two-dimensional system of other studies which is verified by theory [12] and experiments [35].

References

[1] Se Gi Yu, Pevzner V B, Kim K W, Stroscio M A 1998 *Phys. Rev.* B **58** 3580
[2] Sang Chil Lee et al 2005 *Physica* E **28** 402
[3] Bennett C R, Guven K, Tanatar B 1998 *Phys. Rev.* B **57** 3994
[4] Nishiguchi N 1995 *Phys. Rev.* B **52** 5279
[5] Svizhenko A, Balandin A, Bandyopadhyay S, Stroscio M A 1998 *Phys. Rev.* B **57** 4687
[6] Zheng, Matsura M 2000 *Phys. Rev.* B **61** 12624
[7] Ridley B K 1989 *Phys. Rev.* B **39** 5282
[8] Cho Y J, Choi S D 1994 *Phys. Rev.* B **49** 14301

[9] Spector H N, Lee J, Melman P 1986 *Phys. Rev.* B **34** 2554
[10] Weman H, Sirigu L, Karlsson K F, Leifer K, Rudra A, Kapon E 2002 *Appl. Phys. Lett.* **81** 2839
[11] Matthiesen C, Vamivakas A N, Atatre M 2012 *Phys. Rev. Lett.* **108** 093602
[12] Rudin S, Reinecke T L 1990 *Phys. Rev.* B **41** 7713
[13] Bhat J S, Kubakaddi S S, Mulimani B G 1992 *J. Appl. Phys.* **72** 4966
[14] Bhat J S, Kapatkar S B, Kubakaddi S S, Mulimani B G 1998 *Phys. Status Solidi* B **209** 37
[15] Bhat J S, Mulimani B G, Kubakaddi S S 1994 *Phys. Rev.* B **49** 16459
[16] Dinh L, Phuc H V 2015 *Superlattices Microstruct.* **86** 111
[17] Wei B H, Kim C S 1998 *Phys. Rev.* B **58** 9623
[18] Zheng R, Matsuura M 2000 *Phys. Rev.* B **61** 12624
[19] Phuong L T T, Phuc H V, Phong T C 2014 *Physica* E **56** 102
[20] Phong T C, Phuong L T T, Hien N D, Lam V T 2015 *Physica E* **71** 79
[21] Phong T C, Phuc H V 2011 *Mod. Phys. Lett.* B **25** 1003
[22] Phong T C, Phuong L T T, Phuc H V 2012 *Superlattices Microstruct.* **52** 16
[23] Phuong L T T, Phuc H V, Phong T C 2014 *Physica* E **56** 102
[24] Phong T C, Phuong L T T, Phuc H V, Vinh P T 2013 *J. Korean Phys. Soc.* **62** 305
[25] Phuc H V, Hien N D, Dinh L, Phong T C 2016 *Superlattices Microstruct.* **94** 51
[26] Dudley J, Reid D, Sibbett W, Barry L, Thomsen B, Harvey J 1998 *Appl. Opt.* **37** 8142
[27] Bristow A D, Rotenberg N, Van Driel H M 2007 *Appl. Phys. Lett.* **90** 191104
[28] Dupont E, Corkum P, Lui H C, Wilson P H, Buchanan M, Wasilewski Z R 1994 *Appl. Phys. Lett.* **65** 1560
[29] Kojima O, Okumura S, Kita T, Akahane K 2014 *Appl. Phys. Lett.* **105** 181901
[30] Cingolani R, Lepore M, Tommasi R, Catalano I M, Lage H, Heitmann D, Ploog K, Shimizu A, Sakaki H, Ogawa T 1992 *Phys. Rev. Lett.* **69** 1276
[31] Brunner K, Abstreiter G, Bohm G, Tränkle G, Weimann G 1994 *Phys. Rev. Lett.* **73** 1138
[32] Bhat J S, Mulimani B G, Kubakaddi S S 1994 *Phys. Rev.* B **49** 16459
[33] Licari J J, Evrard R 1977 *Phys. Rev.* B **15** 2254
[34] Masale M, Constantious N C 1993 *Phys. Rev.* B **48** 11128
[35] Weber G et al 1991 *Semiconductor Science and Technology* **6** 397